Vertical-cavity surface-emitting lasers with semitransparent metallic mirrors and high quantum efficiencies

Li-Wei Tu, E. Fred Schubert, Rose F. Kopf, George J. Zydzik, Minghwei Hong, S. N. George Chu, and Joseph P. Mannaerts
AT&T Bell Laboratories, 600 Mountain Avenue, Murray Hill, New Jersey 07974

(Received 14 May 1990; accepted for publication 21 August 1990)

Semitransparent thin silver films are employed as both the top mirrors and electrodes for GaAs vertical-cavity surface-emitting lasers. The semitransparent silver films allow the emission of light from the top epitaxial side. Quarter-wave AlAs/$Al_xGa_{1-x}As$ stacks are used as the bottom *n*-type mirrors. Light output versus excitation current measurements yields an efficiency of 0.76 mW/mA from the top silver mirror side, which corresponds to an external differential quantum efficiency of 54% at a lasing wavelength of 0.88 μm. The internal differential quantum efficiency is estimated to be >94%. An optical output power of 10 mW is obtained at a pulsed excitation current of 72 mA.

Vertical-cavity surface-emitting lasers (VCSELs)[1] have a promising future in (i) high-density laser arrays, where two million VCSELs per cm^2 were reported,[2] (ii) high data transmission rate in optical communication systems,[3] and (iii) possibly ultrafast parallel processings in optical computing.[4] In addition, VCSELs could be used for high-speed and high-data transmission between electronic chips.

VCSELs feature light emission along the film growth direction, which is parallel to the direction of the injection current. Due to this feature, the mirror and electrical contact physically occupy the same side of the laser structure, i.e., either on the top or the bottom of the sample. As a result, the design of the mirror/electrode is more complicated as compared to horizontal cavity lasers. The advantages of metallic mirrors are multifold. They offer low series resistance, high thermal conductance, a simplified processing procedure, a planar structure, and serve as an ohmic contact. Silver is chosen as the metallic mirror/contact because of its low electrical resistivity ($\sim 2\times 10^{-6}$ Ω cm at 300 K), good thermal conductivity (~ 4 W cm^{-1} K^{-1} at 300 K),[5] and high reflectivity at wavelengths around 0.87 μm,[6] which corresponds to the bandgap energy of the laser active material GaAs. Continuous-wave operation at room temperature was reported by Schubert *et al.* for thicker silver films.[7]

The $Al_xGa_{1-x}As$/GaAs laser structures are grown in a Varian Gen II molecular beam epitaxy (MBE) system. Heavily doped n^+-type (001) oriented GaAs wafers are used as the substrates. The active region is 0.6 μm lightly doped p^--GaAs with 0.5 μm p^+-$Al_{0.3}Ga_{0.70}As$ on its top and 3 μm n^+-$Al_{0.20}Ga_{0.80}As$ at its bottom as confining layers. A thin, heavily doped p^+-$Al_{0.10}Ga_{0.90}As$ layer is deposited on the very top to facilitate the ohmic contact. The bottom mirror consists of 22.5 pairs of a quarter-wave AlAs/$Al_{0.05}Ga_{0.95}As$ (730 Å/600 Å) multilayer distributed Bragg reflector (DBR). The laser structure was described in detail in a previous publication.[7] Transmission electron microscopy (TEM) micrographs of the laser structure are shown in Fig. 1. Figure 1(a) is the overall laser structure. The uniformity of the GaAs active region and the interface sharpness of the bottom mirror structure are clearly shown in Figs. 1(b) and 1(c), respectively. No graded interfaces are employed in the bottom mirror structure, though stress could remain in the interfaces as indicated in Fig. 1(c). The reflectivity of the DBR structure is checked with a Perkin–Elmer Lambda 9 Spectrophotometer. The reflectivity spectrum shows a broad, high-reflectivity band centered at ~ 0.87 μm with a reflectivity >99%, which matches a calculated reflectivity curve very well. The MBE-grown laser samples are then transferred to a separate high vacuum chamber, where Ag layers with various thicknesses from 300 to 2000 Å are deposited. Standard photolithographic techniques are employed to define circular Ag dots with diameters of 10 and 20 μm. A solution of $3HNO_3$:$4H_2O$ is used to etch the unwanted Ag regions, which leaves a clean, smooth $Al_xGa_{1-x}As$ surface. The final step is to bond the substrate side of the sample on a copper slab with a conductive epoxy. The copper slab serves as a simple, reliable heat sink. Lasers are electrically pumped using a fine probe, and the electroluminescence (EL) spectra are analyzed by a SPEX 1702/04 spectrometer and a GaAs photomultiplier. The light output power of the laser is measured with an

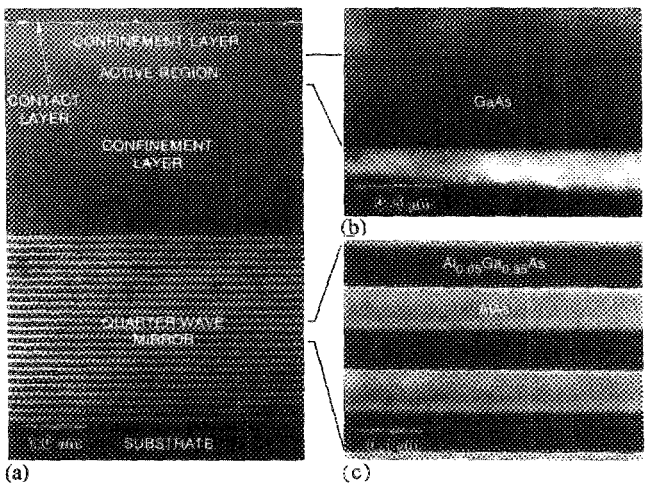

FIG. 1. (a) Overall TEM laser structure, (b) GaAs active region, and (c) bottom mirror structure. Some TEM processing residue is left on the very top of the sample.

 0003-6951/90/462045-03$02.00

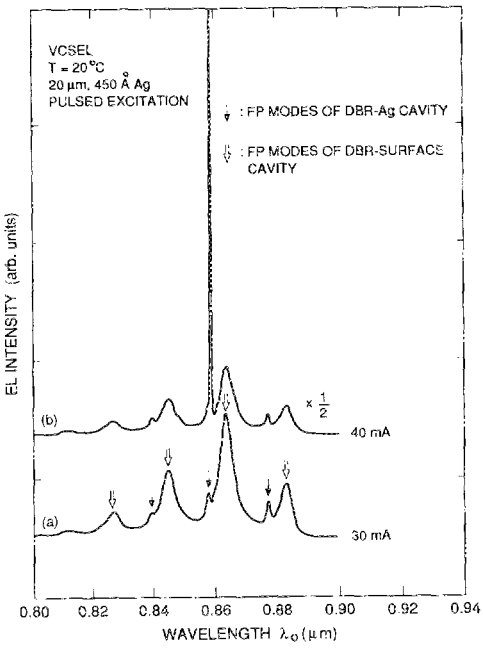

FIG. 2. EL spectra for a 20 μm 450-Å-thick Ag spot (a) below, and (b) above threshold, which is 40 mA.

ANDO AQ-1125 optical power meter calibrated at 0.85 μm. Current-voltage characteristics are checked routinely with a Sony/Tektronix 370 programmable curve tracer. The threshold voltage of the laser diode is $\sim$1.3 V which is close to the energy band gap of GaAs gain medium ($\sim$1.4 eV at room temperature). Above the threshold voltage, the current maintains a linear relation with the forward bias, which gives a differential resistance $\sim$4 Ω for a 20 μm device, indicating that the nonalloyed Ag contact is ohmic.[7] All the measurements are done at room temperature, and no special cooling techniques are employed, such as *p*-side down mounting or substrate thinning.

EL spectra of the VCSEL with a 20-μm-diam Ag spot are shown in Fig. 2. The thickness of the Ag is 450 Å. Figure 2(a) is below lasing threshold. The spectrum is characterized by clear Fabry–Perot (FP) modes. The full width at half maximum (FWHM) of the FP modes is 7.4 Å. Figure 2(b) shows the lasing spectrum above threshold. The width of the lasing peak is 0.1 Å, which is limited by the resolution of the spectrometer. The separation between the FP modes is $\sim$206 Å, which is in good agreement with the nominal FP cavity length of 4.2 μm. The broad peaks, which have the same peak-to-peak distance as that of the much sharper FP modes, are believed due to the spontaneous emission light emitted from the side of the Ag spot. The FWHM of the FP modes for different Ag thicknesses is shown in Fig. 3(a). The peak widths become larger for thinner Ag mirrors. From the finesses of the FP modes, reflectivities for Ag mirrors with different thicknesses are estimated as shown in Fig. 3(b).[8] The reflectivity of the bottom mirror is chosen to be 1 in the calculations. The reflectivity decreases sharply when the Ag thickness is less than $\sim$400 Å. From the FWHM of the broad peak (see Fig. 2), a reflectivity of $\sim$40% is obtained, which is comparable to the reflectivity between GaAs and air. For 2000-

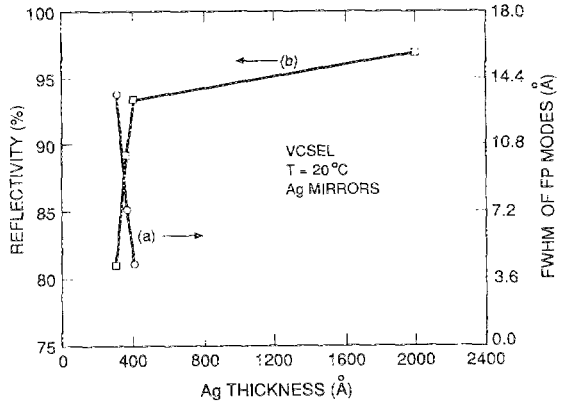

FIG. 3. (a) Measured FWHM of the FP modes the thickness of the Ag mirrors and (b) the calculated reflectivities vs the thickness of the Ag mirrors. Reflectivity of 2000 Å Ag is calculated from the optical constants of Ag.

Å-thick Ag mirrors, only broad peaks are seen, and no sharp FP modes are observed. The reflectivity at 2000 Å Ag thickness shown in Fig. 3(b) is obtained from calculation using the optical data of Ag.[9] Lasing threshold currents under pulsed operation versus the thicknesses of Ag mirrors are shown in Fig. 4. The diameter of the Ag mirrors is 20 μm. The lasing threshold current increases as the Ag mirror thickness decreases. This can be qualitatively explained by the decrease of the reflectivities with decreasing Ag thicknesses [see Fig. 3(b)].

The light output from the top Ag mirror versus pulsed excitation current is shown in Fig. 5. The Ag mirror has a diameter of 10 μm, and is 400 Å thick, with 0.1 MHz, 100 ns injection current pulses applied to the laser diode. In the stimulated emission regime, the output power depends linearly on the excitation current. No power saturation is observed up to the peak powers shown. An optical power of 10 mW is achieved at an excitation current of 72 mA with an operating voltage of $\sim$2.5 V. VCSELs with 300 Å, 20 μm Ag mostly have external differential quantum effi-

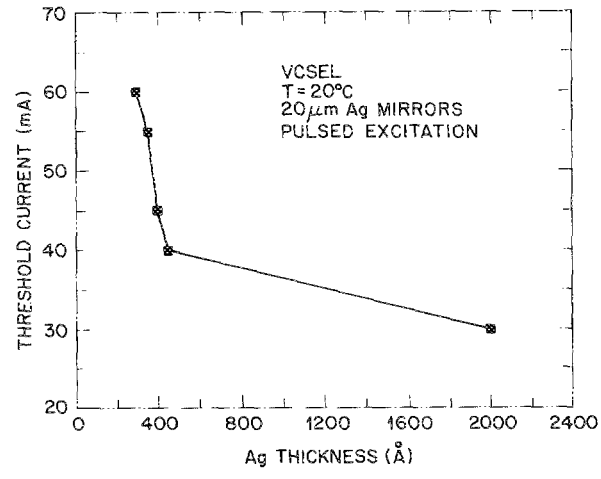

FIG. 4. Lasing threshold currents thicknesses of Ag mirrors. The Ag contact has a diameter of 20 μm.

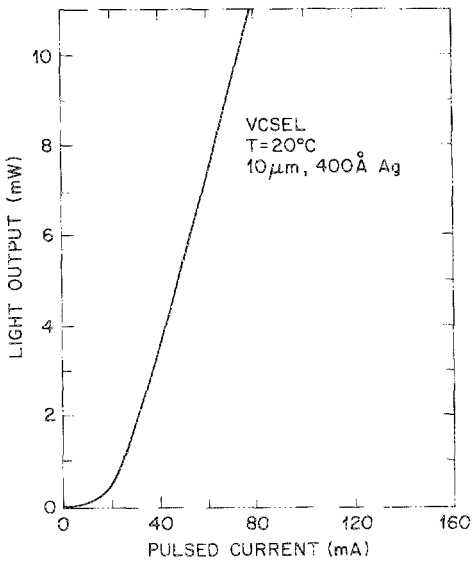

FIG. 5. Light output vs pumping current with a 10-μm-diam, 400-Å-thick Ag spot. The excitation current is 0.1 MHz, 100 ns pulses.

ciencies of 40–50%. Figure 6 is the light output result for a 20 μm, 300 Å Ag spot under 0.1 kHz, 60 ns excitation pulses. The slope near the lasing threshold is 0.76 mW/mA, which yields an external differential quantum efficiency of 54% at a lasing wavelength of 0.88 μm. The operating voltage at 4 mW is ~2.2 V. Note that an external differential quantum efficiency of 15% in Fig. 5 is considerably lower than that in Fig. 6. It is mainly due to (i) the thicker Ag thickness, i.e., larger absorption, and (ii) the smaller Ag diameter, i.e., larger diffraction loss.

Many reasons could restrain the value of the external quantum efficiency, such as current spreading due to the planar nature of the structure, diffraction loss due to the finite size of the mirror, and the absorption due to Ag films. A first-order estimation of the reduction of the external differential quantum efficiency due to the Ag mirror absorption is done on a reflectivity/transmission measurement of a 400 Å Ag film grown on quartz. The measurement reveals that the light intensity transmitted through the 400 Å Ag film approximately equals that absorbed by the Ag film. By multiplying an absorption factor $\exp(-\alpha_{Ag}t)$, which is about 2 for $t = 400$ Å, to the internal differential quantum efficiency in the expression relating the external and internal differential quantum efficiency,[1] an internal differential quantum efficiency of $>94\%$ is estimated from the light output power curve shown in Fig. 6.

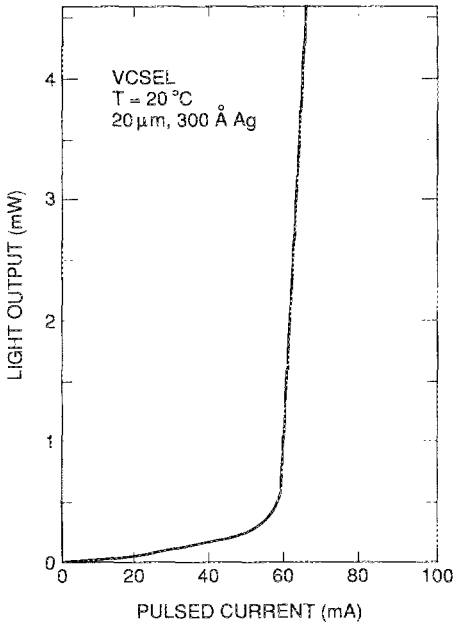

FIG. 6. Light output vs excitation current of 0.1 kHz, 60 ns pulses. The Ag mirror has a diameter of 20 μm, and a thickness of 300 Å.

In conclusion, semitransparent Ag contacts are used in our VCSEL structure. This structure allows light output from the Ag side in a planar configuration. A Ag mirror with a thickness of 300 Å gives a light output efficiency of 0.76 mW/mA. A high external differential quantum efficiency of 54%, and an internal value of $>94\%$ are obtained. A VCSEL with a 400 Å Ag mirror has a light output of 10 mW at a pulsed excitation current of 72 mA. No special cooling is employed. This demonstrates that a suitable metallic reflector such as Ag can play two important roles well in VCSEL, i.e., as an electrode and a mirror, in addition to the other advantages, like high electrical conductivity and low thermal resistance. To lower threshold current densities and achieve continuous-wave operation at room temperature, increased top mirror reflectivity is required, like using the metal/semiconductor hybrid mirror.

The authors would like to thank A. Y. Cho, L. C. Feldman, N. K. Dutta, and D. G. Deppe for their support and valuable discussions. One of the authors (LWT) would like to acknowledge K. Tai for his comments on the linewidth and light output measurements.

[1] K. Iga, F. Koyama, and S. Kinoshita, IEEE J. Quantum Electron. **24**, 1845 (1988).
[2] A. Scherer, J. L. Jewell, Y. H. Lee, J. P. Harbison, and L. T. Florez, Appl. Phys. Lett. **55**, 2724 (1989).
[3] G. P. Agrawal and N. K. Dutta, *Long-Wavelength Semiconductor Lasers* (Van Nostrand Reinhold, New York, 1986), p. 15.
[4] G. A. Evans, N. W. Carlson, J. M. Hammer, M. Lurie, J. K. Bulter, M. Ettenberg, J. Connolly, L. A. Carr, F. Z. Hawrylo, E. A. James, C. J. Kaiser, J. B. Kirk, W. F. Reinhert, S. R. Chinn, J. R. Shealy, and P. S. Zory, *Proceedings of the 11th IEEE International Semiconductor Laser Conference* (IEEE, New York, 1988), p. 166.
[5] C. Kittel, *Introduction to Solid State Physics* (Wiley, New York, 1986), pp. 110, 144.
[6] D. G. Deppe, A. Y. Cho, K. F. Huang, R. J. Fischer, K. Tai, E. F. Schubert, and J. F. Chen, J. Appl. Phys. **66**, 5629 (1989).
[7] E. F. Schubert, L. W. Tu, R. F. Kopf, G. J. Zydzik, and D. G. Deppe, Appl. Phys. Lett. **57**, 117 (1990).
[8] M. Born and E. Wolf, *Principles of Optics*, 6th ed. (Pergamon, New York, 1980), p. 331.
[9] A. V. Sokolov, *Optical Properties of Metals* (Elsevier, New York, 1967), p. 231.